Earth Surface Processes and Landforms
Earth Surf. Process. Landforms **24**, 449–462 (1999)

SIZE DISTRIBUTIONS OF SALTATING GRAINS: AN IMPORTANT VARIABLE IN THE PRODUCTION OF SUSPENDED PARTICLES

DALE A. GILLETTE[1,*] AND WEINAN CHEN[2]

[1]*Atmospheric Sciences Modeling Division, Air Resources Laboratory, National Oceanic and Atmospheric Administration, Research Triangle Park, NC 27711, USA*

[2]*National Research Council, Air Resources Laboratory, National Oceanic and Atmospheric Administration, Research Triangle Park, NC 27711, USA*

Received 6 July 1998; Revised 29 September 1998; Accepted 30 September 1998

ABSTRACT

Size distributions were obtained for airborne particles in the saltation layer for cases where the ratio of the vertical flux of suspended particles to the horizontal flux of particles of all sizes is known. The data can be used to test theories of emissions of suspended particles. All of our sampled erodible soils with textures of sand, loamy sand and loam had saltation-grain mean particle sizes in the range 117–160 μm. Our clay soil had saltation mean particle sizes ranging from 560 to 584 μm. In the light of these data, we interpret the results found previously as supporting sandblasting rather than direct aerodynamic entrainment. The data are consistent with sandblasting theories of Shao *et al.* and of Alfaro. Copyright © 1999 John Wiley & Sons, Ltd.

KEY WORDS: dust; emissions; sandblasting; saltation

INTRODUCTION

Experiments by Shao *et al.* (1993) show that sandblasting of a surface by saltating particles is an important and probably dominating mechanism that produces suspension particle flux. By sandblasting, we mean particle–particle interactions that act to release portions of aggregated particles or to break the crystalline structure of a mineral particle. The Shao *et al.* (1993) expression for the particle flux of suspended particles produced by impact of saltating particles is

$$F_a = K m_d \frac{g}{\Psi} q f\left(\frac{V_H}{u_*}\right) \tag{1a}$$

where Ψ is binding energy, K is a constant, m_d is mass per particle, g is acceleration of gravity, V_H is the horizontal velocity of the saltating particle, u_* is friction velocity, and

$$q = \int_0^\infty C_{salt} V_H(z) dz \tag{1b}$$

Here C_{salt} is the concentration of saltating particles at height z. In Equation 1a K and g are constants and the

* Correspondence to: Dr D. A. Gillette, Atmospheric Sciences Modeling Division, Air Resources Laboratory, National Oceanic and Atmospheric Administration, Research Triangle Park, NC 27711, USA
Email: GILLETTE.DALE@epamail.epa.gov

CCC 0197-9337/99/050449–14 $17.50

function f has been shown by Owen (1964) to be almost constant. Therefore, the ratio F_a/q may be expressed as:

$$\frac{F_a}{q} = K' \frac{m_d}{\Psi} \tag{2}$$

where

$$K' = \left[Kgf\left(\frac{V_H}{u_*}\right)\right]$$

Using Equation 2 to evaluate F_a/q requires evaluation of the binding energies of suspension-sized particles to the soil and the sizes of typical saltation particles. It is an easier task to evaluate the size distribution of saltating particles than it is to evaluate binding energies of the potentially suspended particles in the soil.

An alternative approach has been proposed by Alfaro *et al.* (1997,1998). In their theory, the size distributions of the saltating particles are vitally important because the kinetic energy of individual saltating grains, along with the kinetic energy required to release suspendable particles, determines the quantity and size distribution of the suspended aerosol produced by sandblasting. The kinetic energy required to release suspendable particles in this theory is assumed not to depend on mineralogical composition.

The approaches both of Shao *et al.* (1993) and of Alfaro *et al.* (1997) show that the size distribution of the saltating grains is important. One data set (Gillette *et al.*, 1997) gives F_a/q values for experiments in which the size distribution of saltating particles was measured. These data were for an eroding dry lake floor at Owens Lake, California, USA. The surface sediment was classified as 'loam'. The value for F_a/q was measured to be $5{\cdot}4 \times 10^{-4}$ m^{-1} and the value for F_a/q_{tot} was $2{\cdot}75 \times 10^{-4}$ m^{-1} (see Equation 3 for a definition of q_{tot}).

The purpose of the current paper is to present newly developed size distribution information for saltating particles for experiments where the ratio F_a/q had been measured. The data may then be examined to see if any clear-cut behaviour of F_a/q with size distribution can be observed. The results for the Owens Lake loam soil of Gillette *et al.* (1997) are used in the discussion for comparison. Soils from which the saltating particles originated (parent soils) were processed for size distributions in the same ways as the airborne particles so that a comparison could be made.

DATA EXAMINED FOR SIZE DISTRIBUTION INFORMATION

Sediment samples were saved from experiments reported by Gillette (1981). The samples had been stored in sealed plastic bags and had not been disturbed since weighing them shortly after their collection in the field. The experiments provided measurements of F_a and q_{tot} where q_{tot} is defined by:

$$q_{tot} = \int_0^{75cm} C_{tot} V_H \mathrm{d}z \tag{3}$$

where C_{tot} is the concentration of all airborne particles (mass per volume). F_a values were calculated using the profile method (see Gillette *et al.* (1997) for details). The following are the differences between q and q_{tot}:

- q_{tot} is integrated from the ground level to 75 cm above the ground, whereas q is integrated from the ground to infinity. However, in practice the top of the saltation layer (which contains all saltating particles) is much lower than 75 cm (Owen, 1964).
- q integrates mass from saltating particles only, whereas q_{tot} integrates mass from all particles, saltating, suspended and creeping; q_{tot} includes q. A typical value of q/q_{tot} is 0·513 (Gillette *et al.*, 1997).

Table I. Soil properties of sampled soils in Texas

	Plains/1	Union/2	Bronco/3	Plains/4	White Hill/5	Abernathy/9
Soil moisture(%)	0·52	0·99	1·29	0·41	0·52	6·60
Mass $< 0{\cdot}84$ mm (%)	95·0	98·9	89·1	95·9	98·8	9·3
Vegetative residue ($g\ m^{-2}$)	26·67	8·25	3·67	91·60	19·1	2·90
Ridge roughness (cm)	2·5	2·5	2·5	3·7	2·5	2·5
Erosion fetch (km)	1·6	0·8	1·6	1·6	0·2	0·1
Soil texture	sand	sand	loamy sand	sand	sand	clay
Mass $D > 50$ μm (%)	96·0	95·9	81·5	96·8	93·1	28·0
Mass $50 < D < 2$ μm (%)	0·5	1·0	8·5	1·4	1·0	20·0
Mass $D < 2$ μm (%)	3·5	3·5	10·0	1·8	5·9	52·0

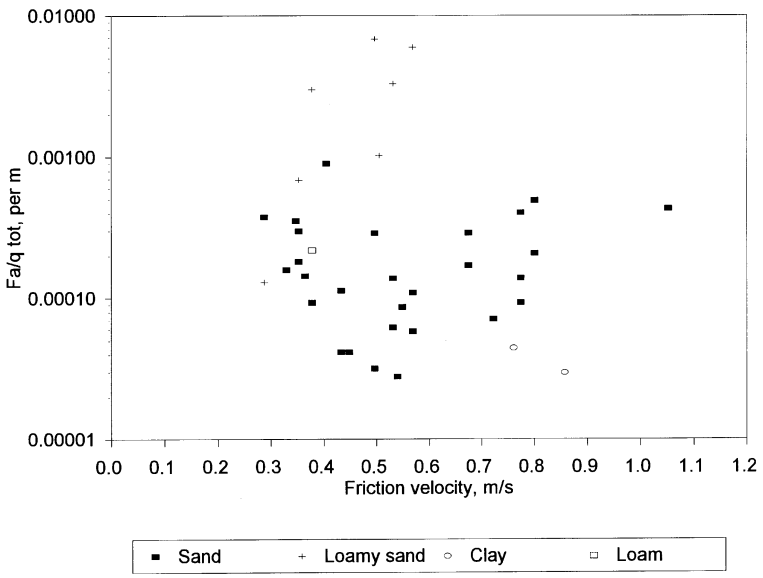

Figure 1. Values of F_a/q_{tot} (m^{-1}) versus friction velocity ($m\ s^{-1}$) for the data sets described in the text for sand, loamy sand, clay and loam textures (after Gillette *et al.*, 1997)

The samples from which q_{tot} values were calculated were all sampled using a Bagnold catcher described by Gillette and Goodwin (1974). The catcher collected airborne particulate mass fluxing into the height intervals 0–1, 1–15, 15–30, 30–45, 45–60 and 60–75 cm, referred to as height intervals 1–6, respectively. The eroding soils were in western Texas, USA (Bronco/3, Plains/1 and 4, Union/2, White Hill/5 and Abernathy/9). Soil textures are given in Table I along with other erosion parameters. The value of q_{tot} was the total mass of particles collected at a given height interval divided by the time interval of collection. The sampling was done so that conditions of wind speed were constant during the times of collection (typically 20 min to 1 h). The samples were all obtained when wind speed was greater than threshold for wind erosion and the soil was dry.

A plot of the F_a/q_{tot} data is given in Figure 1. The individual values were aggregated into three groups by surface texture of the parent soil:

- Sand: Plains/1, Plains/4, Union/2 and White Hill/5 (all in Yoakum County, Texas, USA, except for Union/2 in Terry County).
- Loamy sand: Bronco/3 (Yoakum County, Texas, USA).
- Clay: Abernathy (Hale County, Texas, USA).

By far the largest number of samples, representing four sites, was for sand textures. The other textures are represented by one site each. The 'sand' textures suggest a fairly constant range of F_a/q_{tot} values. This range of F_a/q_{tot} values for a wide range of u_* supports a sandblasting mechanism for the emission of fine particles from sand soils if the size of the saltating particles is similar for all the samples, along with the distribution of the binding energies (see Equation 2). Loamy sand F_a/q_{tot} values are mostly higher than the sand values and the clay values are smaller than the sand values. For comparison, the loam F_a/q_{tot} value from the Owens Lake, California, experiment (see above) is in the same range as the 'sand' samples.

EXPERIMENTAL DETAILS

The 62 samples were processed in the same structure and composition as when they were sampled. The individual samples came from six height intervals at 11 individual collections taken at the six sites. Four of the highest interval samples were too small to use. The instrument for size distribution determination was the Vertical Settling Aerosol Tube (VSAT) method (Fryrear *et al.*, 1998). Samples were separated in a splitter to 0·03–0·05 g except for a few that were small and could only be processed in less than 0·03 g. These quantities were previously determined to be optimal for VSAT analysis. The VSAT is a device for measuring size distribution of aerosol particles by sedimentation in air. It has a sample-release system at the top of a vertical glass tube that is 6·0213 m in length, and a sample receiving, weighing and recording system at the bottom. Both systems are connected to a computer. The release system disperses samples into the vertical tube, then the catcher system measures the accumulation of sediment by weight at the base of the tube every 0·001 s.

Settling velocity is calculated by the Navier Stokes law. Three forces acting on a free-falling particle in still air can be described by:

$$m\frac{dV}{dt} = mg - m'g - \frac{\rho_p A}{2} C_d V^2 \tag{4}$$

where m is mass of a falling particle (kg), m' is immersed weight of a falling particle (kg), g is acceleration due to gravity (m s^{-2}), V is falling velocity (m s^{-1}), ρ_p is density of particle (kg m^{-3}), taken as 2600 kg m^{-3} in this calculation, A is projection area of a particle (m^2) and C_d is a drag coefficient that varies with the Reynolds number, R_e, where:

$$R_e = \frac{\rho_a V d}{\mu} \tag{5}$$

Here V is settling velocity (m s^{-1}), d is particle diameter (m) and ρ_a is density of air (kg m^{-3}):

$$\rho_a = 0 \cdot 041206 \times 5 \cdot 155 \times 10^2 \times \left(\frac{P}{T}\right) \tag{6}$$

where P is air pressure (inches of Hg) and T is temperature (in °R, which equals (°C + 273) × 1·8) measured at the top, the middle and the bottom of the tube. The absolute viscosity of a fluid, μ (kg s^{-1} m^{-1}) is given by:

$$\mu = \frac{\beta T^{1.5}}{T + S} \tag{7}$$

where $\beta = 1{\cdot}458 \times 10^{-6}$ (kg s^{-1} m^{-1} K$^{-1/2}$), T is absolute temperature (K) and S is the Southerland constant, 110·4 K. When $R_e < 1$, the process can be treated as a Stokes' fluid in which $C_d = 24/R_e$; when $R_e > 1$ Fair and Geyer (1963) found that Equation 8 can be used for calculating the drag coefficient of a sphere settling in

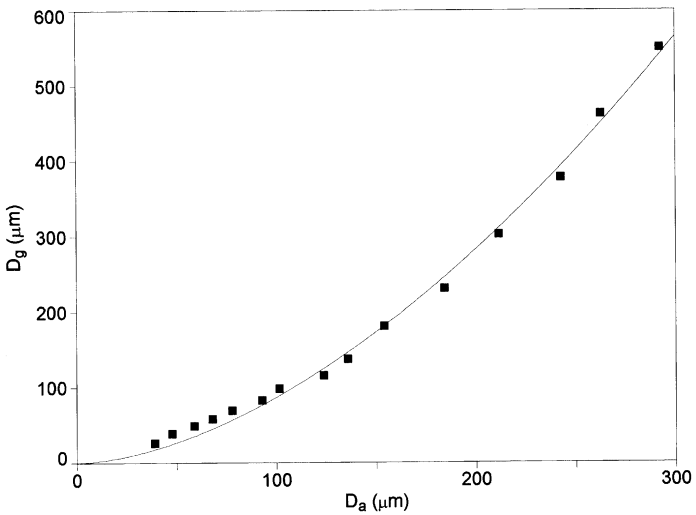

Figure 2. Comparison between aerodynamic diameters D_a (obtained using the VSAT) and geometric diameters D_g (measured) using glass spheres with uniform diameters and densities. $D_g = 0{\cdot}033\ D_a^{1{\cdot}7068}$; $r^2 = 0{\cdot}995$

a fluid with a wide range of Reynolds number: $0{\cdot}5 \leq R_e \leq 10^4$:

$$C_d = \frac{24}{R_e} + \frac{3}{R_e^{0{\cdot}5}} + 0 \cdot 3 \tag{8}$$

Since humidity has little influence on density and viscosity of the air when it is lower than 50 per cent, it is neglected in this calculation. The settling velocities of particles are calculated for 1 μm intervals in diameter from 10 μm to 1000 μm. Because the motion equation of falling particles cannot be resolved explicitly, the settling velocity and position of each size of a falling particle are calculated by a short interval Δt of 0·001 s. The drag coefficient and absolute viscosity are calculated according to the air temperature at different heights. A particle reaches its terminal velocity when:

$$\frac{dV}{dt} = 0 \tag{9}$$

Calculations are repeated until the particle falls through the tube's length of 6·0213 m. The calculated time for each size of particle that falls through the tube and reaches the scale at the bottom of the tube is compared with the recorded cumulative weight for each 0·001 s so that the time distribution for falling particles of a sample can be converted to an aerodynamic size distribution.

In practice, we converted the aerodynamic size distributions to geometric size distributions similar to those obtained by sieving. Since many size distributions are done by sieving, it is worthwhile to show how size distributions done by the two methods may be compared. We did a series of experiments with glass spheres of measured geometric diameters and particle densities. Samples of the glass spheres were checked microscopically for sphericity. The relationship between the geometric diameter D_g and aerodynamic diameter D_a is shown in Figure 2. The figure shows that the aerodynamic size distribution is compressed compared with the geometric size distribution: $D_a/D_g > 1$ for $D_g < 100$ μm and $D_a/D_g < 1$ for $D_g > 100$ μm. A regression analysis of the aerodynamic size distribution versus the geometric size distribution for glass

spheres gave the following relationship:

$$D_g = 0 \cdot 033 D_a{}^{1 \cdot 7068} \tag{10}$$

For the regression the explained variance $r^2 = 0 \cdot 995$ and significance level is 0·001. Equation 10 was used to convert the aerodynamic size distributions into geometric size distributions. It should be remembered that this conversion is strictly correct only for spherical particles of the density of glass. Soil particles are irregular and may have a density that is slightly different from that of glass, so slight errors would be expected for some soils. Six samples were processed by the sieving method using ultrasonic sieves to check the converted VSAT data. They were: Union/2, sample 17, height intervals 1 and 2; Union/2, sample 20, height intervals 1 and 2; and White Hill/5 sample 17, height intervals 1 and 2. The ratio of the converted mass mean diameter obtained by the VSAT to that obtained by sieving was $0 \cdot 85 \pm 0 \cdot 09$.

The distribution of grain-size parameters of each sample was calculated by a graphic method suggested by Folk and Ward (1957). On the basis of the cumulative frequency polygon, the 5th, 16th, 25th, 50th, 75th, 84th and 95th percentiles can be obtained by a computer program, and the parameters can be calculated from the following

Graphic mean diameter:

$$(\phi_{16} + \phi_{50} + \phi_{84})/3 \tag{11}$$

Inclusive graphic standard deviation:

$$(\phi_{84} - \phi_{16})/4 + (\phi_{95} + \phi_5)/6 \cdot 6 \tag{12}$$

Inclusive graphic skewness:

$$(\phi_{16} + \phi_{84} - 2\phi_{50})/(2\phi_{84} - \phi_{16}) + (\phi_5 + \phi_{95} - 2\phi_{50})/(2\phi_{95} - \phi_5) \tag{13}$$

Graphic kurtosis:

$$(\phi_{95} - \phi_5)/2 \cdot 44(2\phi_{75} - \phi_{25}) \tag{14}$$

where ϕ is a unit of grain size (McLane, 1995):

$$\phi = \log_2(d/d_0) \tag{15}$$

where d is the diameter (in mm) and d_0, a reference grain size, is fixed at 1 mm:

$$D_\phi = -1 \cdot 4427 \ln(D_{mm}) \tag{16}$$

where D_ϕ is the particle diameter (in ϕ units) and D_{mm} is the particle diameter (in mm). After calculations are made in ϕ units, the mass mean diameter values are converted into millimetres.

RESULTS

Size distributions for each height interval of the Bagnold catcher (see above) were chosen for three texture classes: sand (Figure 3), loamy sand (Figure 4) and clay (Figure 5). Figure 3 is subdivided into seven subfigures showing histogram size distributions for seven individual experiments. The figures show for the particular soils sampled that the size distributions of the airborne particles ($50\ \mu m < D_g < 1000\ \mu m$) are

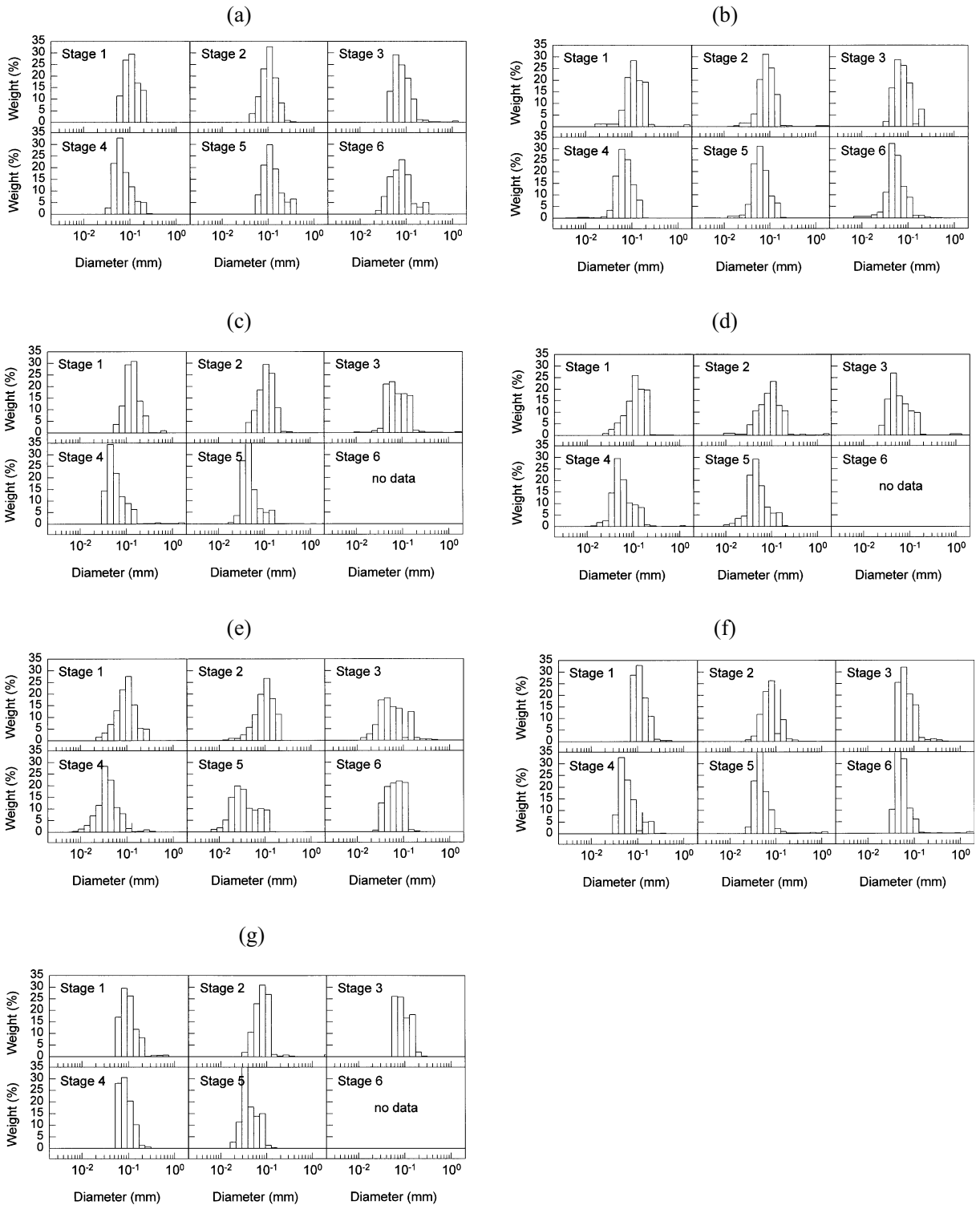

Figure 3. Histograms of percentage of weight versus geometric diameter for sand soils: (a) Plains/1, sample no. 14; (b) Plains/1, sample no. 15; (c) Union/2, sample no. 17; (d) Union/2, sample no. 20; (e) Plains/4, sample no. 12; (f) White Hill/5, sample no. 17; (g) White Hill/5 sample no. 18. Stages refer to height intervals 1 to 6 (defined in text)

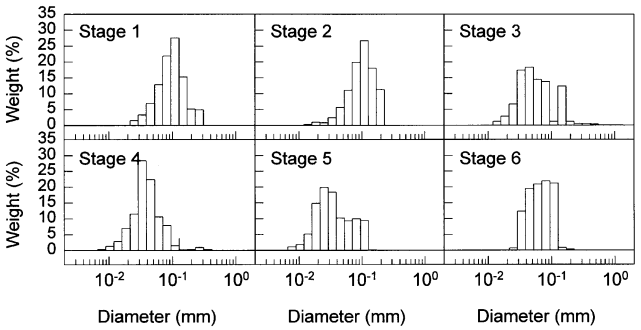

Figure 4. Histograms of percentage of weight versus geometric diameter for a sandy loam soil: Bronco/3, sample no. 1. Stages refer to height intervals 1 to 6 (defined in text)

rather well described as lognormal distributions having single modes. Table II summarizes the size distributions for each height interval for all the samples. For clay samples where particle sizes were too large to be in the practical range for VSAT testing, size distributions were done by sieving and the standard deviations and skewness were not computed (both were set to zero). Since saltating particles have roughly parabolic trajectories, the saltation layer may be identifiable as that layer above which the mass flux decreases rapidly and in which the size distribution of particles is roughly the same. For example, Figure 3 shows that sand-textured soils at height interval 1–3 (the first 15 to 30 cm) had roughly the same relative size distribution. Above height interval 3 (30 cm) the size distributions were usually depleted in the largest particles. In addition, the mass catches for the same intervals were much reduced. We interpreted this to show the existence of the saltation layer in the first 15 to 30 cm. Figure 4 shows for a loamy sand soil that the saltation layer height (using the same interpretation as above) extends to 30 cm for the conditions of the experiment. Figure 5 shows size distributions for clay sediments. These distributions show a much larger size, corresponding to a threshold velocity that was much larger than for any of the other soils used in this paper. The clay soils in Table II also show mass catches that decrease less rapidly with height up to the top of the measuring device at 75 cm. Therefore, the clay soils represent material more resistant to breakup. The two criteria of consistency of size distribution and mass flux (data given in Table II) were used to estimate the height of the saltation layer as summarized in Table III. The average of the mass mean diameters of the samples within each saltation layer were calculated to provide an estimate of the mean particle size within the saltation layer (Table III).

Size distributions for the 'parent soils' of the airborne particles collected by the Bagnold Catcher are shown in Figure 6. The soils are shown by location. The Plains 1973 and 1974 are the Plains /1 and /4 referred to above. The figures suggest lognormal distributions having single modes for the soil particles (50 μm $< D_g <$ 1000 μm) for the Plains 1973 site and for the Union site. For the Bronco, Plains 1974 and White Hill, the data suggest two modes for the size range (50 μm $< D_g <$ 1000 μm). Table IV summarizes the size distributions for each parent soil sample. Figure 7 shows a size distribution obtained by sieving of the Randall clay soil for the Abernathy site. This soil sample was obtained at the time of the Abernathy Bagnold catcher samples. This size distribution shows a seeming lognormal distribution having a mode at about 2 mm. Also shown in this figure are microphotographs of the particles showing rather straight edges for the 2 mm particles and more rounded smaller particles.

DISCUSSION AND CONCLUSION

It was surprising to the authors that the many different erodible soils with textures of sand and loamy sand had saltation-grain mean particle sizes in the range 106–144 μm. The clay soil had saltation mean particle sizes ranging from 574 to 592 μm. Thus for this limited sampling of particles only the clay soils had markedly different mean saltating particle sizes.

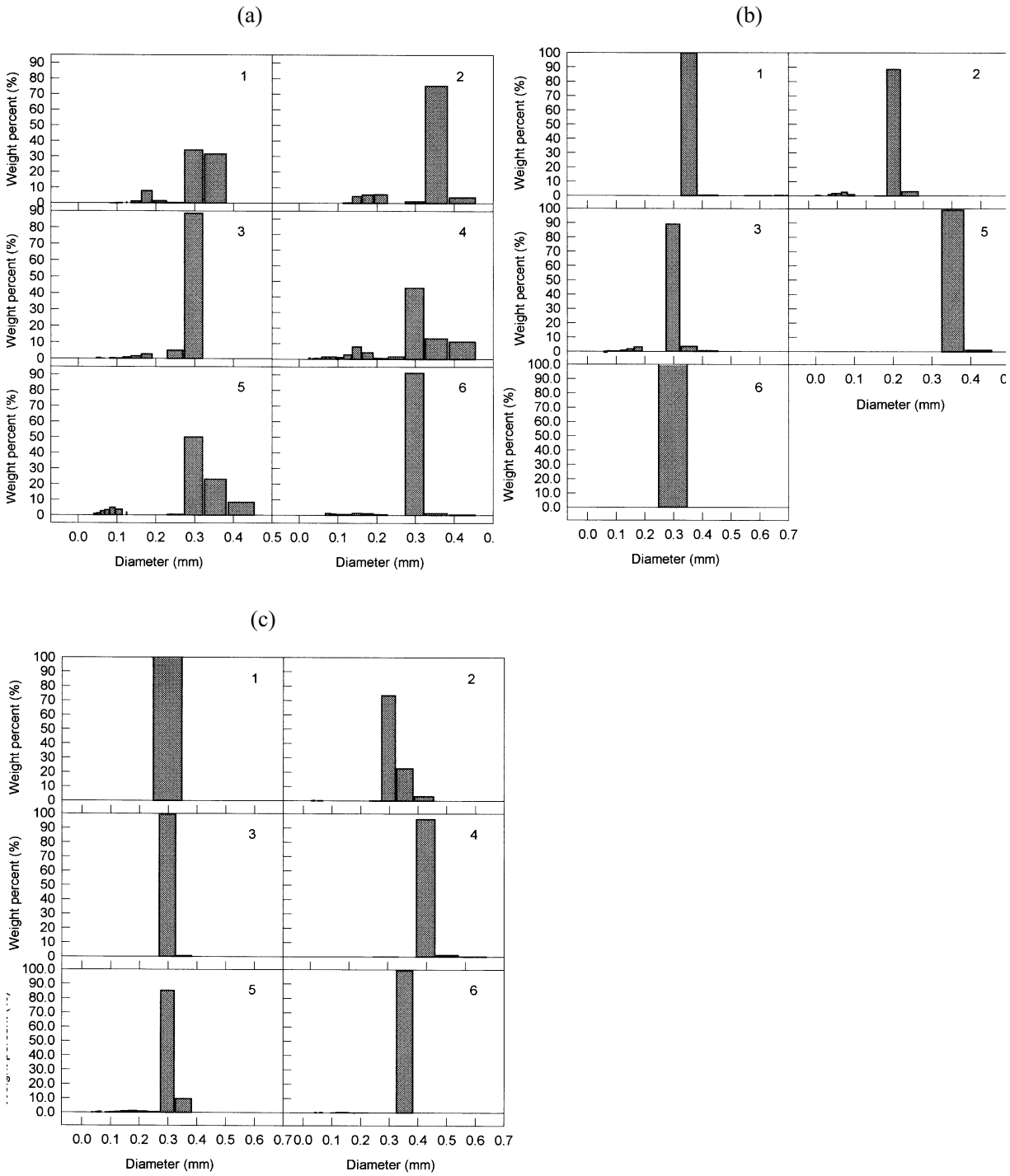

Figure 5. Histograms of percentage of weight versus geometric diameter for a clay soil: (a) Abernathy/9 sample no. 1; (b) Abernathy/9 sample no. 2; (c) Abernathy/9 sample no. 3. Numbers 1 to 6 refer to height intervals (defined in text)

Table II. Mass of particles collected for each height interval, geometric mean diameter, geometric standard deviation, skewness and kurtosis for the eroding soil samples

Place/Soil	Height Int.	Collected mass (g)	Geometric mean D (μm)	Geometric std dev.	Skewness	Kurtosis
Plains/1 (sample 14)	1	88·82	139·9	0·538	−0·16	1·04
	2	16·82	136·1	0·510	0·05	1·03
	3	0·75	105·5	0·555	−0·11	0·84
	4	0·24	94·1	0·616	−0·35	1·09
	5	0·12	91·0	0·683	−0·28	1·27
	6	0·30	97·9	0·686	−0·05	1·20
Plains/1 (sample 15)	1	227·48	158·2	0·672	−0·13	0·92
	2	121·09	116·3	0·512	0·04	0·98
	3	42·05	100·1	1·894	−0·31	1·92
	4	16·48	93·9	0·543	−0·07	0·96
	5	9·39	86·4	0·569	−0·19	1·15
	6	5·13	75·3	0·573	−0·17	1·15
Union/2 (sample 17)	1	380·25	175·3	0·497	−0·01	1·02
	2	36·58	143·7	0·511	0·17	0·96
	3	1·09	104·4	0·621	−0·07	0·68
	4	0·39	78·7	0·620	−0·36	0·91
	5	0·22	65·7	0·641	−0·41	1·33
Union/2 (sample 20)	1	607·64	148·5	0·560	0·19	1·04
	2	31·67	121·5	0·743	0·12	0·93
	3	33·36	80·0	0·754	−0·24	0·90
	4	16·58	79·0	0·731	−0·33	0·97
	5	9·38	67·2	0·719	−0·22	1·22
Bronco/3 (sample 1)	1	22·53	112·6	0·678	0·05	1·12
	2	4·10	126·1	0·678	0·08	1·22
	3	0·56	82·6	0·803	−0·11	0·87
	4	0·40	52·6	0·771	−0·06	1·18
	5	0·20	49·9	0·952	−0·22	0·82
	6	0·11	88·5	0·608	0·07	0·79
Plains/4 (sample 12)	1	232·84	161·1	0·670	−0·11	0·91
	2	137·02	125·1	0·605	0·04	1·06
	3	41·89	120·3	0·696	0·04	0·97
	4	13·75	99·2	0·622	−0·06	1·03
	5	6·96	92·2	0·691	−0·12	1·34
	6	4·05	73·5	0·517	0·02	0·81
White Hill/5 (sample 17)	1	15·13	146·6	0·486	−0·2	0·95
	2	2·91	106·5	0·531	0·09	0·93
	3	0·63	90·3	0·518	−0·22	0·85
	4	0·30	84·6	0·656	−0·35	0·97
	5	0·30	64·8	0·528	−0·26	1·17
	6	0·18	73·3	0·454	−0·22	1·24
White Hill/5 (sample 18)	1	33·32	126·3	0·574	−0·12	1·09
	2	3·16	106·8	0·470	0·06	0·92
	3	0·15	114·5	0·548	−0·14	0·77
	4	0·08	107·6	0·473	−0·06	0·83
	5	0·13	57·6	0·431	−0·29	0·85
Abernathy/9 (sample 1)	1	0·12	837·7			
	2	0·25	573·7			
	3	0·41	615·0			
	4	0·29	460·8			
	5	0·13	403·1			
	6	0·12	501·4			
Abernathy/9 (sample 2)	1	13·51	616·4			
	2	33·75	592·3			
	3	36·59	653·1			
	5	17·50	496·8			
	6	9·60	562·4			
Abernathy/9 (sample 3)	1	0·23	606·1			
	2	0·09	579·5			
	3	0·73	642·2			
	4	0·49	478·1			
	5	0·38	536·1			
	6	0·13	515·8			

Table III. Height of the saltation layer (to nearest 15 cm) and mass mean diameter for the eroding soils collected in stage 2 and friction velocity during collection

Place/Soil	Sample no.	Ht of saltation layer(cm)	Mass mean $D(\mu m)$	u_* (ms^{-1})
Plains/1	14	15	136	0·38
Plains/1	15	30	116	0·33
Union/2	17	15	144	0·24
Union/2	20	30	122	0·77
Bronco/3	1	15	126	0·23
Plains/4	12	30	125	0·77
White Hill/5	17	15	106	0·55
White Hill/5	18	15	107	0·5
Abernathy/9	1	75	574	0·76
Abernathy/9	2	75	592	0·54
Abernathy/9	3	75	580	0·85

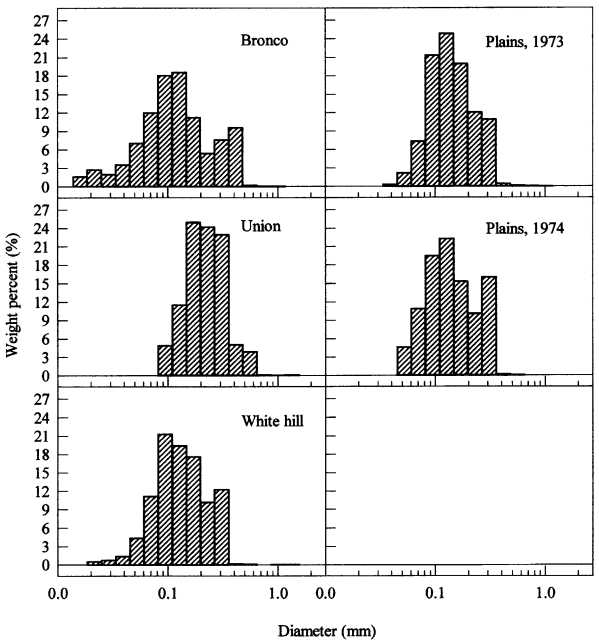

Figure 6. Histograms of percentage of weight versus geometric diameter for parent soils. The Plains 1973 and 1974 are the same as Plains /1 and /4 in the text. The other locations are the same as the locations where the airborne particles were collected by the Bagnold catcher

Table IV. Geometric grain-size distribution parameters of the surface soils

Sample	Mean diameter (μm)	Std dev.	Skewness	Kurtosis
Bronco	143·1	1·129	−0·060	1·172
Plains 1973	163·0	0·652	−0·166	0·952
Union	242·3	0·641	−0·126	1·172
Plains 1974	163·3	0·802	−0·145	0·908
White hill	151·6	0·753	−0·066	0·965

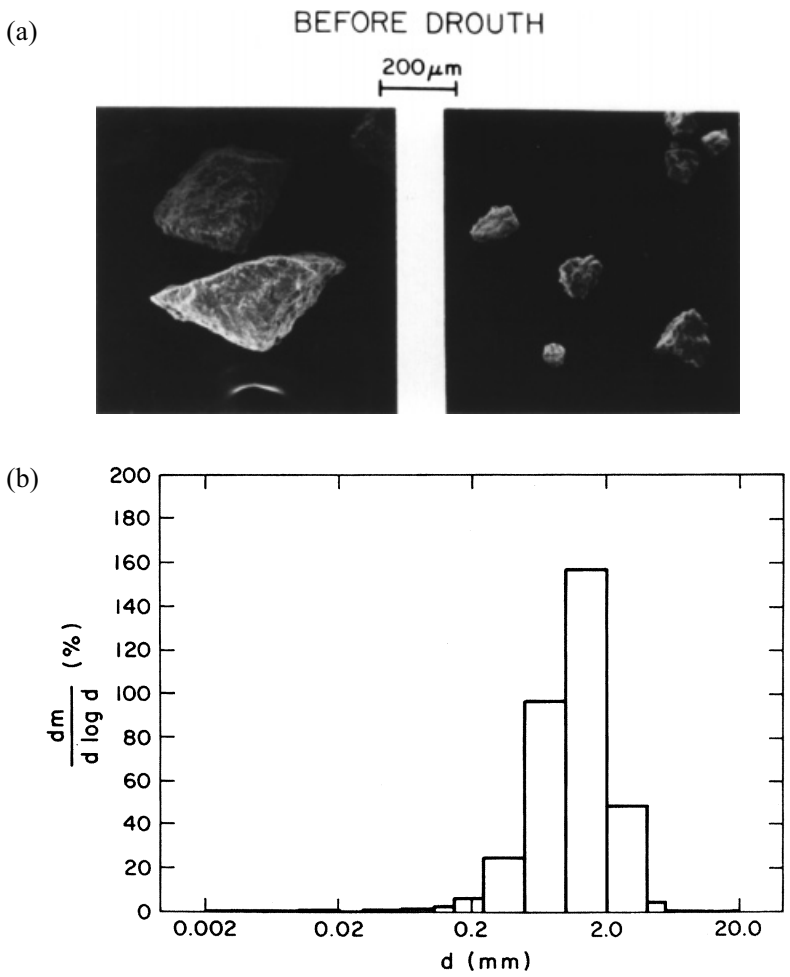

Figure 7. Scanning electron micrographs of particles and size distribution of loose surficial particles of a Randall clay soil at Abernathy TX (after Gillette, 1997)

We interpret the measurement for F_a/q_{tot} for loam (a texture having abundant fine particles) being in the same range as for sand (a texture not abundant in fine particles) as supporting sandblasting rather than direct aerodynamic entrainment. The size distribution for the Owens Lake loam soil measured is shown in Figure 8 (Gillette *et al.*, 1997). This size distribution also shows an abundance of saltation-grain mean particles in the range 117–160 μm. Measurements were consistent with but not precisely the same as the methods used for the present study. In contrast with the size distributions in Figures 3–5 for sand, loamy sand and clay soils which suggest lognormal size distributions having single modes, the loam texture shows a size distribution that strongly suggests three modes. This multiplicity of modes is consistent with the results from Chatenet *et al.* (1996) and Alfaro *et al.* (1998) who used a three-mode lognormal distribution to describe the general soil size distribution of particles of size 50 $\mu m < D_g < 1000$ μm. It is probable that the generalized particle size distribution for particles in that size range has from one to at least three modes and that the soils for our experiment represent a subset of these soils. Since the size distribution of the loam texture of Gillette *et al.* (1997) is trimodal, a single mass mean diameter is not useful and the full size distribution information should be used.

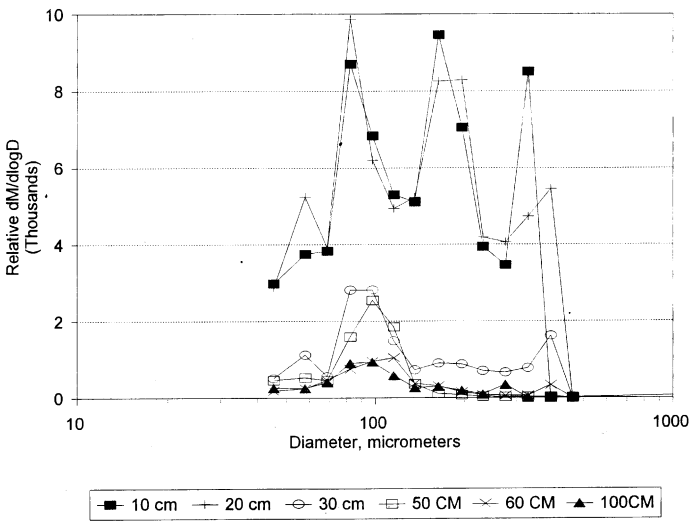

Figure 8. Size distribution of horizontal particle flux for loam sediment: Owens Lake, California, 11 March 1993. Relative units of dM/d log D are (mass/area) (after Gillette *et al.*, 1997)

Alfaro *et al.*'s (1998) theory coupled with the errors in determining friction velocities and mass fluxes offers an explanation for the wide variety of F_a/q_{tot} values found in our data within a single texture type. The simpler theory of Shao *et al.* (1993) does not seem to explain the wide variability of F_a/q_{tot} for our sand surface texture data. Noting the simplicity and similarity of the size distributions for the seven sand soils examined here, we would expect from the Shao *et al.* theory that F_a/q_{tot} values would be less scattered if the binding energies for suspended particles were similar for all the sampled sand soils. It is possible, however, that the seemingly, randomly scattered F_a/q_{tot} values are caused by experimental variability. Although it is possible that other models might also explain the data (a fairly constant range of F_a/q_{tot} vs. u_* for similar size distributions of saltating particles in the sand texture), we presently see the data as consistent with a sandblasting mechanism for dust production. If a constant ratio of fine particles to sand-sized particles were to be specified in the vertical flux F_a then the ratio F_a/q_{tot} as a function of u_* would be expected to significantly decrease as u_* increases, since the saltation hop distance increases with u_*.

For the loamy sand soil, F_a/q_{tot} values are higher than seen for sand soils, but the size distribution of the saltating particles (Figure 4) is similar to those for the sand. Gillette and Walker (1977) showed scanning electron microscope photographs for one of the sand-textured soils and for the loamy sand used in this paper. The microstructures of the soil particles for the sand soils and for the loamy sand soils were very different. The sand soils were quartz particles coated with particles that could be released by sandblasting. Although the particles were not spherical, they were irregular and not elongated or dendritic. The loamy sand particles were dendritic, having extremely complicated structures (like those of snow flakes). It is possible that there were many differing binding energies in the loamy sand that combined to increase F_a/q_{tot} as friction velocity increased. Nonetheless, this dendritic structure does not mean that particle–particle interactions are not necessary to emit fine particles. It only means that there is a wider range of binding energies for some soils than for others.

Our clay aggregates were also analysed using scanning electron microscopy (Gillette, 1977) to show that individual grains were almost cubical and smooth. The size distributions (Figure 7) show that the cubical aggregates were also of fairly uniform size. Since the mass for an individual clay saltating grain is very great compared with that for individual saltating grains for the sand soils above, and because the threshold velocity for saltation was high, the kinetic energy delivered per saltating grain was very high. The low values for F_a/q_{tot} in Figure 1 imply that the binding energy of clay soils is high (consistent with the Alfaro's *et al.* (1996) hypothesis). The hypothesis of high binding energies is supported by studies of the size distribution and

morphology of the clay aggregates at the beginning and end of a season of high winds and wind erosion. After a period of windy drought the surface clay aggregates were only slightly rounded by impacts and their size distribution decreased from a mode of close to 2 mm to a mode of about 0·3 mm (Gillette, 1977).

For the loam texture class the F_a/q_{tot} values fell into the range of the sand soils. Because only one value at one friction velocity was recorded, however, little evidence was given on the binding energy. It is likely that the threshold binding energy for some of the suspendable particles of the loam soil is similar to that for sand. Because of the complexity of the loam size distribution, however, it is likely that the F_a/q_{tot} values vary with friction velocity.

Finally, comparison of the size distributions of parent soils with the airborne particles shows that the single-mode soils (Plains/1 and Union) have quite similar size distributions for the lowest height interval of the Bagnold Catcher and the parent soils. For the soils having a suggestion of two modes (Bronco, Plains/2 and White Hill), the airborne particles are depleted in the largest sizes of the soil size distributions and so appear to have single-mode distributions.

REFERENCES

Alfaro, S. C., Gaudichet, A., Gomes, L. and Maille, M. 1997. 'Modeling the size distribution of a soil aerosol produced by sandblasting', *Journal of Geophysical Research*, **102**, **D10**, 11,239–11,249.

Alfaro, S., Gaudichet, A., Gomes, L. and Maille, M. 1998. 'Mineral aerosol production by wind erosion: aerosol particle sizes and binding energies', *Geophysical Research Letters*, (submitted).

Chatenet, B., Marticorena, B., Gomes, L. and Bergametti, G. 1996. 'Assessing the actual grain-size distributions of desert soils erodible by wind', *Sedimentology*, **43**, 901–911.

Fair, G. M. and Geyer, J. C. 1963. Water Supply and Waste Water Disposal, John Wiley & Sons, New York.

Folk, R. L. and Ward, W. C. 1957. 'Brazos River bar, a study in the significance of grain-size parameters', *Journal of Sedimentary Petrology*, **27**, 3–27.

Fryrear, D. W., Xiao, J. B. and Gillette, D. A. 1998. 'Aerodynamic equivalent diameter of particles using VSAT', *Sedimentology*

Gillette, D. 1981. 'Production of dust that may be carried great distances', in Pe'we',T., (Ed.), Desert Dust: Origin, Characteristics, and Effect on Man, Geological Society of America, Special Paper 187, 11–26.

Gillette, D. A. 1977. 'Fine particulate emissions due to wind erosion', *Transactions of the American Society of Agricultural Engineers*, **20**, 890–897.

Gillette, D. A. and Goodwin, P. A. 1974. 'Microscale transport of sand-sized soil aggregates eroded by wind', *Journal of Geophysical Research*, **79**, 4080–4084.

Gillette, D. A. and Walker, T. R. 1977. 'Characteristics of airborne particles produced by wind erosion of sandy soil, high plains of West Texas', *Soil Science*, **123**, 97–110.

Gillette, G. A., Fryrear, D. W., Gill, T. E., Ley, T., Cahill, T. A. and Gearhart, E. A. 1997. 'Relation of vertical flux of particles smaller than 10 μm to total aeolian horizontal mass flux at Owens Lake', *Journal of Geophysical Research*, **102D**, 26,009–26,016.

McLane, M. 1995. Sedimentology, Oxford University Press, New York.

Owen, P. R. 1964. 'Saltation of uniform sand grains in air', *Journal of Fluid Mechanics*', **20**, 225–242.

Shao, Y., Raupach, M. R. and Findlater, P. A. 1993. 'The effect of saltation bombardment on the entrainment of dust by wind', *Journal of Geophysical Research*, **98D**, 12719–12726.

